

## 11. Instrumentation and Technique

### 11-1. Avalanche Photodiode Detector for Observing Nuclear Excitation on $^{197}\text{Au}$ in K-Shell Ionization

Avalanche photodiode (APD) detectors for synchrotron X-ray experiments have been developed at the Photon Factory. An APD detector can also detect electrons having energies of between 1-100 keV even though the detection layer of the APD is relatively thin (several 10  $\mu\text{m}$  thick). Its properties of sub-nanosecond time resolution and high count-rate capability are kept even in detecting electrons. Recently, an electron detector using a silicon APD was developed and applied to the observation of Nuclear Excitation by Electron Transition (NEET) on  $^{197}\text{Au}$  [1]. NEET occurs during atomic inner-shell ionization if the nuclear and electron transitions have nearly the same energy and a common multipolarity. NEET on  $^{197}\text{Au}$  can be observed between the  $\text{K} \rightarrow \text{M}_1$  hole transition ( $1\text{S}_{1/2}$ : 80.725 keV  $\rightarrow$   $3\text{S}_{1/2}$ : 3.425 keV) and the  $3/2^+ \rightarrow 1/2^+$  nuclear transition ( $0 \rightarrow$  77.351 keV, half-life: 1.91 ns). The common multipolarity is  $\text{M}1$ . It has been difficult to observe NEET due to its small probability. There was a large difference between the theoretical and experimental values of the NEET probability, which is defined as the probability of nuclear excitation per ionization. For  $^{197}\text{Au}$ , only one experiment was ever known. The experimental NEET probability was  $5.1 \times 10^{-5}$  [2] while the calculated value was  $1.3 \times 10^{-7}$  [3].

We have developed a time spectroscopy system with a silicon APD to observe internal-conversion electrons emitted from excited nuclei. By recording a decay curve of the internal conversion electrons in ionizing gold atoms, we can prove whether NEET occurs. Through tests of the detector system in time and energy spectroscopy executed at BL-14A, we designed the APD device and decided on some parameters for its operation. An experiment for observing NEET on  $^{197}\text{Au}$  was carried out at BL09XU

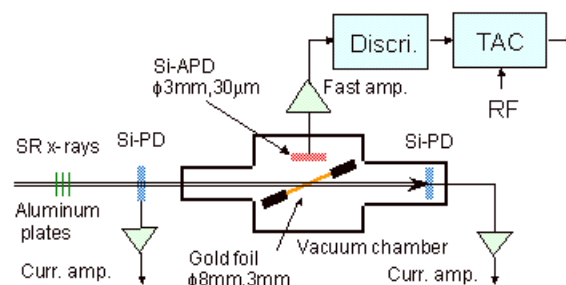


Figure 1. Experimental setup for the NEET observation.

at SPring-8. Figure 1 illustrates the experimental setup. The third-order X-rays from a Si(111) double-crystal monochromator were used to tune the energies in the 77-81 keV region. The X-ray beam was passed to a vacuum chamber, in which a gold target and an APD were installed. A pair of silicon PIN photodiodes monitored the beam intensity. The radiation emitted from the target was detected by the APD having a sensitive region of 3 mm in diameter and a depletion layer 30  $\mu\text{m}$  thick. The signals from the APD were processed by a fast amplifier and a discriminator. A time spectrum of 20-ns range was recorded with a time-to-amplitude converter using signals from the discriminator and from the accelerator in a 116-bunch mode. Pulses caused by atomic processes piled up in one huge pulse per one bunch. Moreover, their count-rate reached  $10^7 \text{ s}^{-1}$ . The huge prompt pulses were therefore inhibited by the timing system so as not to affect recording a time spectrum of weak conversion electrons.

Figure 2(a) shows a time spectrum measured for NEET. The energy of the incident X-rays was 80.989 keV, higher than the K-edge level of 80.725 keV. The spectrum of Fig. 2(b) was measured at 80.415 keV, which shows a background for Fig. 2(a), since K-shell ionization cannot occur. Figure 2(c) shows the background-subtracted spectrum. A fitted exponential decay curve is shown by the red line in Fig. 2(c). The lifetime given by the curve satisfied  $t = 2.76$  ns for the 77.3-keV nuclear level within error. By

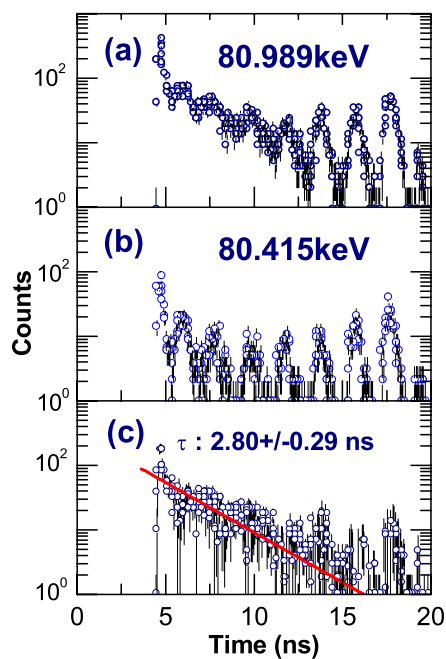


Figure 2.

Time spectra measured (a) for NEET at 80.989 keV, (b) for the background at 80.415 keV. The spectrum (c) was obtained by subtracting (b) from (a).

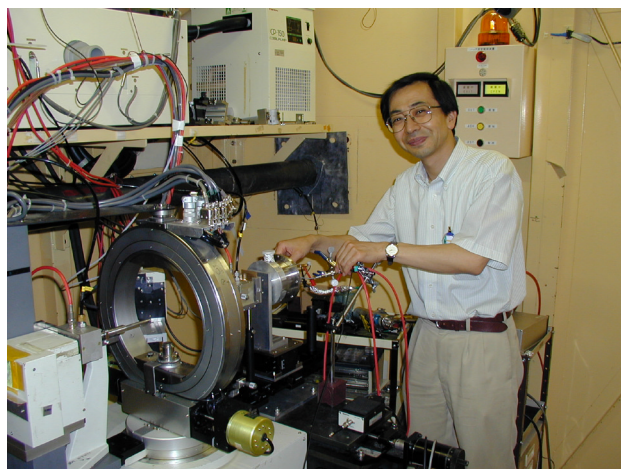
tuning the X-ray energy, we also observed nuclear resonance at 77.351 keV with the same setup as in the NEET measurement. We were able to determine the NEET probability from the event ratio between the nuclear resonance and NEET. The NEET proba-

bility was  $(5.0 \pm 0.6) \times 10^{-8}$ . This value is much closer to a recent calculation. We are now preparing experiments to understand the details of the NEET process.

S. Kishimoto (KEK-PF)

#### References

- [1] S. Kishimoto, Y. Yoda, M. Seto, Y. Kobayashi, S. Kitao, R. Haruki, T. Kawauchi, K. Fukutani and T. Okano, *Phys. Rev. Lett.* 83 (2000) 1831.
- [2] A. Shinohara, T. Saito, K. Otozai, H. Fujioka and K. Ura, *Bull. Chem. Soc. Jpn.* 68 (1995) 566.
- [3] E. V. Tkalya, *Nucl. Phys. A539* (1992) 209.



### 11-2. Polarization-Contrast Imaging with Hard X-Rays

Polarization-contrast imaging in the hard X-ray spectral range (above 2 keV) was performed. The experimental setup consisted of an X-ray polarizer, double diamond phase retarders, and an X-ray CCD detector, as shown in Fig. 1 [1]. The synchrotron white X-ray beam was monochromated and horizontally polarized in the vicinity of the K-absorption edge of an atom of interest by the X-ray polarizer. The monochromated and horizontally polarized X-rays were incident on double-phase retarders. By adjusting the double-phase retarders carefully, the polarization state of the X-rays transmitted by the phase retarders was switched between horizontal- and vertical- linear polarization or right- and left- circular polarization. The polarized X-rays which transmitted the sample were incident on the CCD detector. After image processing to remove the effect of the sample thickness, we successfully observed images result-

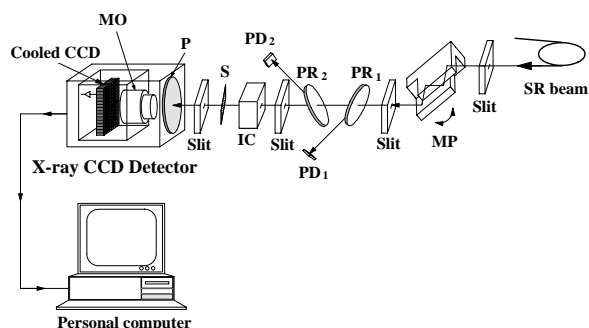


Figure 1.

Experimental setup for acquiring images resulting from X-ray magnetic linear dichroism (XMLD). SR: synchrotron radiation, MP: silicon 331 monochromating polarizer.  $PR_1$  and  $PR_2$ : first and second diamond 111 phase retarders.  $PD_1$ : PIN photodiode monitoring X-rays reflected by the first phase retarder.  $PD_2$ : PIN photodiode monitoring X-rays reflected by the second phase retarder. IC: ionization chamber monitoring X-rays incident to a sample. S: sample. P: phosphor screen. MP: magnifying optical lens.

ing from X-ray natural linear dichroism [2] and from X-ray magnetic circular dichroism [3].

Here, we report on the imaging of the magnetic domains on magnetic tape based on the effect of X-ray magnetic linear dichroism (XMLD) [4]. The sample used was a metal-particulate (MP) magnetic recording medium, which was commercially available. It had an iron-rich magnetic layer with a thickness of  $3.5 \mu\text{m}$  deposited on a carbon-based film, and was held in thirty sheets. We then drew a magnetic pattern on the sample, as shown in Fig. 2, so that 90-degree magnetic domains were made on the sample. The thick arrows in Fig. 2 show the magnetization directions drawn on the sample.

Prior to imaging experiments, we measured the XMLD spectra at the X-ray energies in the vicinity of the iron K-absorption edge (7111 eV). The XMLD spectra (Fig. 3) exhibited the largest positive and negative peaks (about 0.0006 in the relative absorption difference) at photon energies of 7126 eV and 7133 eV as a result of the XMLD effect. Therefore, we chose these X-ray energies for the XMLD imaging experiment.

Figure 4(a) shows the polarization-contrast images arising from XMLD at a photon energy of 15 eV above the iron K-absorption edge. Contrast between 90-degree magnetic domains was clearly observed. The contrast in the image (Fig. 4(b)) was reversed at a photon energy of 22 eV above the

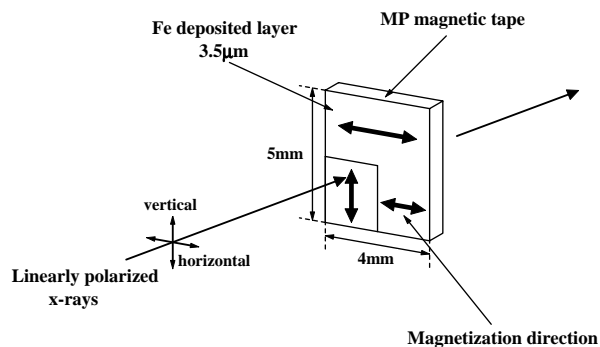


Figure 2.

Schematic arrangement of the sample. The thick arrows indicate the magnetization direction drawn on the tape.

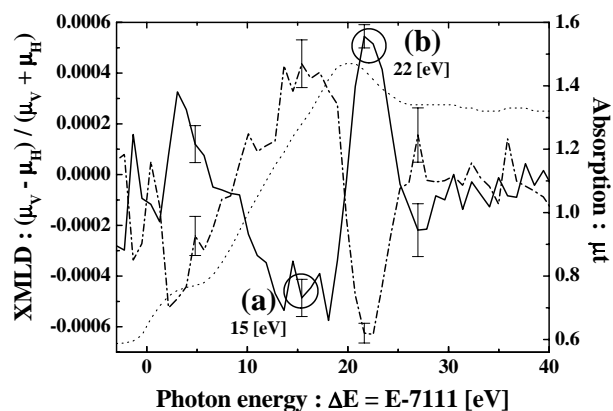


Figure 3.

X-ray magnetic linear dichroism (XMLD) spectra of the metal-particulate (MP) magnetic recording medium at around the iron K-absorption edge (7111 eV). The dotted line indicates the total absorption spectrum.

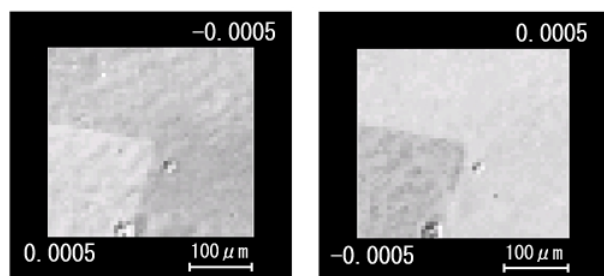


Figure 4.

Images resulting from the X-ray magnetic linear dichroism (XMLD) in the sample of Fig. 3. (a) an image taken at 15 eV, (b) an image taken at 22 eV above the iron K-absorption edge (7111 eV) after the correction against the non-uniformity of the sample thickness. The area size of the image is  $303 \mu\text{m} \times 317 \mu\text{m}$ .

iron K-absorption edge. In order to make a quantitative comparison, we calculated the XMLD values in the respective areas. They are 0.0005 and  $-0.0005$

in Fig. 4(a) and are reversed in Fig. 4(b). All of the above values are consistent with those obtained from the XMLD spectra. Hence, it is concluded that these contrasts originate from differences in the magnetization directions of the sample, namely, originating from the effect of the XMLD in the MP magnetic recording tape.

K. Sato, K. Okitsu, Y. Ueji and Y. Amemiya (Univ. of Tokyo)

#### References

- [1] K. Sato, Y. Hasegawa, K. Kondo, K. Miyazaki, T. Matsushita, and Y. Amemiya, *Rev. Sci. Instrum.* 71 (2000) 4449.
- [2] K. Sato, K. Okitsu, Y. Ueji, T. Matsushita, and Y. Amemiya, *J. Synchrotron Rad.* 7 (2000) 368.
- [3] K. Sato, Y. Ueji, K. Okitsu, T. Matsushita, and Y. Amemiya, *J. Synchrotron Rad.* 8 (2000) 1021.
- [4] K. Sato, Y. Ueji, K. Okitsu, T. Matsushita, J. Saito, T. Takayama, and Y. Amemiya, submitted to *Phys. Rev. B*.

